NeuroImage: Clinical 15 (2017) 483–493

Contents lists available at ScienceDirect

NeuroImage: Clinical

journal homepage: www.elsevier.com/locate/ynicl

Ventricular shape and relative position abnormalities in preterm neonates

N. Paquette[a,1], J. Shi[b,1], Y. Wang[b], Y. Lao[a], R. Ceschin[c], M.D. Nelson[a], A. Panigrahy[c,1], N. Lepore[a,*,1]

[a] Department of Radiology, University of Southern California and Children's Hospital of Los Angeles, CA, USA
[b] School of Computing, Informatics, and Decision Systems Engineering, Arizona State University, Tempe, AZ, USA
[c] Department of Radiology, Children's Hospital of Pittsburgh UPMC, Pittsburgh, PA, USA

ARTICLE INFO

Keywords:
Prematurity
Multivariate tensor-based morphometry (mTBM)
Relative pose
Lateral ventricles
Putamen
Thalamus

ABSTRACT

Recent neuroimaging findings have highlighted the impact of premature birth on subcortical development and morphological changes in the deep grey nuclei and ventricular system. To help characterize subcortical microstructural changes in preterm neonates, we recently implemented a multivariate tensor-based method (mTBM). This method allows to precisely measure local surface deformation of brain structures in infants. Here, we investigated ventricular abnormalities and their spatial relationships with surrounding subcortical structures in preterm neonates. We performed regional group comparisons on the surface morphometry and relative position of the lateral ventricles between 19 full-term and 17 preterm born neonates at term-equivalent age. Furthermore, a relative pose analysis was used to detect individual differences in translation, rotation, and scale of a given brain structure with respect to an average. Our mTBM results revealed broad areas of alterations on the frontal horn and body of the left ventricle, and narrower areas of differences on the temporal horn of the right ventricle. A significant shift in the rotation of the left ventricle was also found in preterm neonates. Furthermore, we located significant correlations between morphology and pose parameters of the lateral ventricles and that of the putamen and thalamus. These results show that regional abnormalities on the surface and pose of the ventricles are also associated with alterations on the putamen and thalamus. The complementarity of the information provided by the surface and pose analysis may help to identify abnormal white and grey matter growth, hinting toward a pattern of neural and cellular dysmaturation.

1. Introduction

Studies using conventional MRI techniques such as volumetric or morphometric analyses have highlighted structural irregularities in cortical and subcortical grey matter in preterm infants. For instance, volumetric decreases were measured within the orbitofrontal and cingulate cortices, the anterior temporal lobe, the thalamus, and the hippocampus of infants and children born prematurely (Isaacs et al., 2000; Kesler et al., 2004; Maalouf et al., 1999; Nosarti et al., 2002, 2008). These structural abnormalities have been shown to persist well into adolescence and adulthood (Allin et al., 2004, 2011; Counsell et al., 2008; Nosarti et al., 2002, 2008, 2014; Skranes et al., 2007; Woo Nam et al., 2015). More recently, brain imaging studies have highlighted the impact of premature birth on subcortical development and morphological changes in the deep grey nuclei. Volumetric reduction in the thalamus and globus pallidus, as well as altered hippocampal shape, were measured in prematurely born children (Boardman et al., 2010; Thompson et al., 2013). In Ball et al. (2012), the degree of prematurity was associated with reduced volume of the thalamus, which predicted overall cortical volume decreases (Ball et al., 2012). Ventricular enlargement has also been frequently documented. In preterm-born adults, significant volumetric increase was a strong predictor for overall volumetric decrease in subcortical grey matter and periventricular white matter (Allin et al., 2004). Similarly, larger ventricular volume on MRI at neonatal equivalent age was correlated with several structural abnormalities in the frontal lobes, cerebellum, brainstem, basal ganglia and thalami (Maunu et al., 2009). Ventricular enlargement might thus contribute to abnormal patterns of grey and white matter development, and heighten the risk of adverse outcomes in preterm infants. However, conventional volume-based MRI analysis still lack in precision and specificity when characterizing subcortical changes in neonates. Innovative ways to evaluate morphological subcortical data in preterm neonates are needed to provide more specific phenotypic neuromarkers of their cerebral development. To our knowledge, few studies have

* Corresponding author at: Department of Radiology, University of Southern California & Children's Hospital Los Angeles, 4650 Sunset Blvd, Los Angeles, CA 90027, USA.
E-mail address: nlepore@chla.usc.edu (N. Lepore).
[1] Equal contribution.

http://dx.doi.org/10.1016/j.nicl.2017.05.025
Received 5 April 2017; Received in revised form 24 May 2017; Accepted 26 May 2017
Available online 28 May 2017

aimed at precisely quantifying and localizing regions of ventricular enlargement and their relation to surrounding cerebral structures abnormalities.

We recently implemented a multivariate tensor-based method (mTBM) to measure local surface deformations of brain structures in preterm children (Shi et al., 2013b; Shi et al., 2012; Wang et al., 2010; Wang et al., 2011b). This method showed greater detection power of structural brain alterations in preterm neonates without major visible brain injury compared to the more traditional univariate version of tensor-based morphometry (Shi et al., 2013b; Wang et al., 2010; Wang et al., 2011c). Complementary to the morphometry analysis, we implemented a relative pose algorithm to measure in translation, rotation, and scale changes of a given brain structure, after removing the effect of the size and alignment of the patient's head within the scanner (Bossa and Olmos, 2006; Bossa et al., 2011a, 2011b; Lao et al., 2014a, 2014b). In this regard, the relative pose analysis offer important information about the anatomical changes in terms of the size, location and orientation of a structure within the brain (Bossa et al., 2011a, 2011b). This type of change is most likely to reflect the impact of diffuse alterations or abnormal growth within both the white and the grey matters (Back, 2015; Back and Miller, 2014).

In previous works, morphological changes were located using mTBM within the anterior and inferior portion of the putamen, and the ventral portion of the thalamic nuclei (Lao et al., 2014b; Shi et al., 2013b). Furthermore, broader left than right difference, suggesting a left vulnerability to preterm birth. Significant shifts in the relative position of the left thalamus and the two putamen were also observed (Lao et al., 2014b; Shi et al., 2013b). Here, to further investigate a left vulnerability of subcortical development in preterm neonates, we extend our methods to the analysis of the left and right ventricles. To characterize the subcortical growth pattern in preterm infants, we perform a correlation analysis of the ventricular surfaces and pose parameters with that of the putamen and thalamus described in Lao et al. (2014b) & Shi et al. (2013b).

2. Materials and methods

2.1. Neonatal sample

Our sample included 17 preterm neonates prospectively recruited with clinically acquired neonatal MRI, and 19 healthy full-term born neonates. Demographic information and birth data of the sample are displayed in Table 1. Demographic data were compared between group using SPSS version 24 (SPSS Inc., Chicago, IL, USA). The group difference in the birth weight was assessed using a parametric *t*-test for independent samples. Non-parametric Mann-Whitney *U* tests were performed on categorical (gender) or non normally distributed variables (Apgar scores at 1 and 5 min, gestational age, and postnatal age at testing). Structural MR images were qualitatively classified by a board certified neonatal neuroradiologist. To be included in the preterm group, infants had to meet the following criteria: 1) fewer than 37 gestational weeks at birth, and 2) visually normal scans on conventional MRI. Participants were excluded based on abnormal neurological exam, or if they exhibited brain lesions including 1) focal or diffuse white matter injury, 2) intra-ventricular hemorrhage I-IV, 3) ventriculomegaly, and 4) significant increase of the subarachnoid space and/or sulcal enlargement.

Table 1
Neonatal characteristics.

	Preterms (n = 17)	Full-terms (n = 19)	Significance
Gestational age	32.80 (3.85)	39.08 (1.25)	$U < 0.001$, $p < 0.001$
Gender [F; M; N/A]	7; 9; 1	9; 8; 2	$U = 123.5$, $p = 0.657$
Birth weight (g)	1849.36 (784.81)	3434.38 (965.54)	$t = 4.70$, $df = 25$, $p < 0.001$
Apgar (1 min)	7.50 (2.22)	6.89 (1.83)	$U = 35$, $p = 0.447$
Apgar (5 min)	8.80 (0.42)	8.56 (0.73)	$U = 38$, $p = 0.604$
Postnatal age at testing (in days)	7.19 (7.09)	6.44 (4.90)	$U = 160$, $p = 0.975$

Mean and (SD in parentheses) unless stated otherwise.

Postnatal age at testing included corrected age for preterm infants (tested at term-equivalent age).

N/A = missing data.

This study was approved by the Children Hospital Los Angeles Committee on Clinical Investigations and the University of Pittsburgh Internal Review Board. Written consent for use of each child's MRI data and for participation in additional neurodevelopmental and neuroimaging studies were obtained from the parents on behalf of the patients by a research coordinator. The ethics committee approved this consent process. As this study involved a retrospective review of all clinically acquired neonatal data for the period between 2005 and 2011, which included neonates who were not enrolled into prospective studies, approval was also obtained from the CHLA Committee on Clinical Investigations and the University of Pittsburgh Internal Review Board for the retrospective use of all neonatal MRI data clinically acquired at CHLA between 2005 and 2011.

2.2. MRI acquisition and pre-processing

MR images were acquired with a dedicated neonatal head coil on a 1.5 T GE scanner, with a coronal 3D SPGR sequence (TE = 6 ms, TR = 25 ms, FOV = 18 cm, Matrix = 256 × 160), axial and sagittal T1-weighted FLAIR sequences (TE = 7.4 ms, TR = 2100 ms, TI = 750, FOV = 20 cm, Matrix = 256 × 160) and an axial T2-weighted FSE sequence (TE = 85 ms, TR = 5000 ms, FOV = 20 cm, Matrix = 320 × 160 or 256 × 128). The scans were optimized for the best grey and white matter contrast, both at the cortical and at the subcortical levels.

T1-weighted MRI scans were registered to a common template space through linear registration, aligned to the MNI space. Each image was bias and motion corrected, and pre-segmented through a neonatal pipeline. The subcortical structures were manually edited by an experienced pediatric neuro-radiologist using the Insight Toolkit's SNAP program (Yushkevich et al., 2006). The intra-rater overlap for measuring the lateral ventricles was 0.88 in four participants (two preterm and two term-born participants) at two subsequent times spanning several months. Ventricular surfaces were reconstructed from the segmented images using a topology-preserving level set method (Han et al., 2003) and represented as triangular meshes using the marching cube algorithm (Lorensen and Cline, 1987). To reduce the noise in the image acquisition and the partial volume effects, we then applied a smoothing process to all subcortical surfaces, consisting of mesh simplification with “progressive meshes” (Hoppe, 1996) and refinement with Loop subdivision surface (Loop, 1987). The smoothed surfaces are accurate approximations of the original surfaces with higher resolution and less noise (Shi et al., 2013a).

2.3. Topology optimization and surface parameterization

For the branchy ventricular surfaces, three cuts were introduced; as shown in Fig. 1a, one cut γ_1 on the superior horn, one cut γ_2 on the occipital horn, and one cut γ_3 on the inferior horn. The cuts were automatically traced by locating the extreme points on the ventricular surface, i.e., the most anterior point, the most posterior point, and the most inferior point in the standard template space. According to the protocol described in (Chollet et al., 2014), these are consistent and meaningful landmarks of the lateral ventricles. We also ensured that the cuts have the same directions and lengths across subjects. By slicing open along the cuts, each ventricular surface is modeled as a genus-0 surface with three open boundaries. We call this process topology

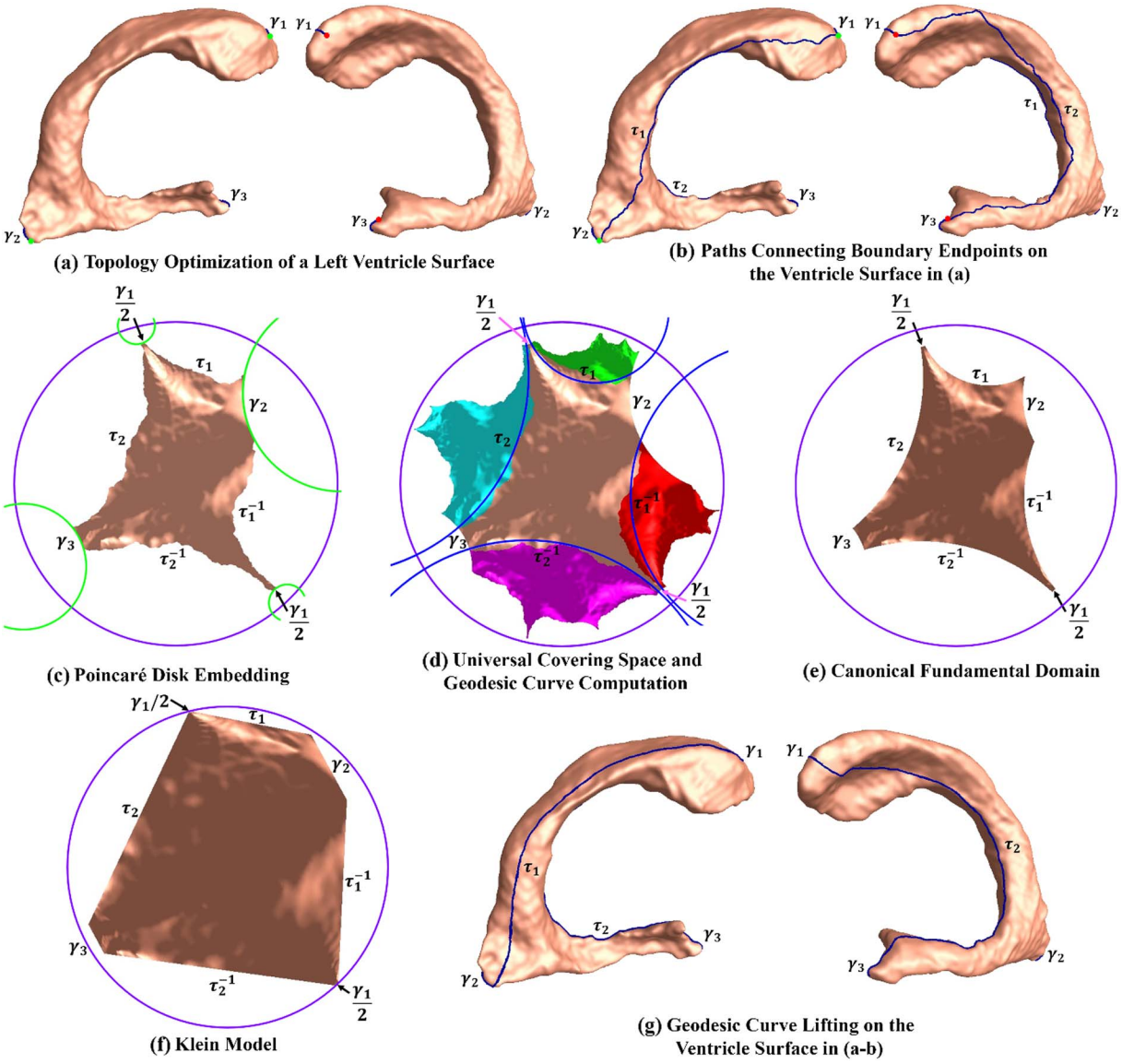

Fig. 1. Computation steps in the proposed ventricular morphometry registration.

optimization (Shi et al., 2015; Shi et al., 2013a; Wang et al., 2010; Wang et al., 2011c).

For the surface registration, we computed a conformal parameterization using the Hyperbolic Ricci Flow method (Shi et al., 2015). The ventricular surfaces resulting from topology optimization admit hyperbolic geometry and their conformal parameterizations can be efficiently computed with this method (Hamilton, 1988; Shi et al., 2015; Zeng et al., 2010). It is a general and powerful tool to compute surface conformal parameterization based on the correspondence between the surface Riemannian metric and the Gaussian curvature i.e., when the surface metric changes, the Gaussian curvature will change accordingly. The hyperbolic Ricci flow allows to compute conformal parameterizations for general topological surfaces (i.e., high-genus surfaces or genus-0 surfaces with more the two open boundaries) with minimal angle distortions and no singular points. With the conformal parameterization, a 3D ventricular surface can be embedded onto the 2D Poincaré disk. For embedding, each ventricular surface is sliced open along the three cuts and two paths τ_1 and τ_2, which connect γ_1 and γ_2, γ_1 and γ_3, respectively, as shown in Fig. 1b. The Poincaré disk embedding of a ventricular surface is illustrated in Fig. 1c. For details about hyperbolic Ricci flow and Poincaré disk embedding, please refer to (Shi et al., 2015).

2.4. Ventricular surface registration

As shown in Fig. 1c, the three cuts become geodesics (hyperbolic lines) in the Poincaré disk. However, the two paths, where each splits into two identical segments τ_i and ${\tau_i}^{-1}, i = 1, 2$, are not geodesics and not consistent across subjects. For ventricular surface registration, the locations of the paths need to be determined. In the Poincaré disk, we use the Fuchsian group generators (Shi et al., 2015) to tile a finite portion of the universal covering space, i.e. the whole Poincaré disk, of each ventricular surface, as shown in Fig. 1d. In the universal covering space, we recompute the locations of the paths as unique and consistent geodesic curves. By slicing the universal covering space along the new paths, we obtain the canonical fundamental domain of a ventricular surface, as shown in Fig. 1e. These new geodesics, when lifted to original 3D ventricular surfaces, are also consistent (Fig. 1g) and can be used as boundary conditions of the surface registration. Finally, we convert the canonical fundamental domain to the Klein model, as shown in Fig. 1f. The Klein model is used as the canonical parameter domain to register each ventricular surface to a common template. Please refer to (Shi et al., 2015) for details of the ventricular surface registration algorithm.

2.5. Multivariate tensor-based morphometry

We used multivariate tensor-based morphometry (mTBM) (Lepore et al., 2008; Wang et al., 2008) to measure ventricular surface deformations that occur in the registration process. First, the Jacobian matrix (J) is computed at each vertex from the transformation between the population-based template and the subject's shape. The logarithm of the deformation tensor matrix $\log \sqrt{JJ^T}$ is used to measure local differences on a brain structure morphology with respect to the population shape (Arsigny et al., 2006; Lepore et al., 2008; Wang et al., 2010). Multivariate statistics on the deformation tensor in the Euclidean space have been shown to improve group effect sizes, thus increasing statistical power (Shi et al., 2013b; Wang et al., 2010; Wang et al., 2011c). Furthermore, we applied the heat kernel smoothing algorithms (Chung et al., 2005) to increase the signal-to-noise-ratio (SNR) and improve the sensitivity of the statistical analysis. As in (Shi et al., 2013b), we covaried the smoothed mTBM measure to correct for post-conception age effects, by applying a general linear model.

Group differences on mTBM were computed vertex-wise using the multivariate Hotelling's T^2 test, which is a multivariate generalization of the t-test (Hotelling, 1931). Permutation tests (10, 000) were used to correct for multiple comparisons (Nichols and Holmes, 2002). We used the group comparison p-map to visualize the shape morphometry patterns between the two groups. These p-values are computed by comparing the data to a permutation distribution in order to eliminate the assumption of normal distribution. The whole structure-based permutation corrected p-value was used to measure the overall significance of the p-map at the 0.05 alpha level. Furthermore, to see the direction of changes between groups, we mapped the det$J$ matrix at each vertex k in a ratio map according to the following formula:

$$R^k = \frac{\sum_j^{N1} det J_{1i}^k}{\sum_j^{N2} det J_{2j}^k} \frac{N_2}{N_1} \quad (1)$$

where ${J_{1i}}^k$ and ${J_{2j}}^k$ are the Jacobian matrices for ith subject in one group and jth in the other group, and N_1 and N_2 are the number of subjects in each groups (Shi et al., 2013a; Wang et al., 2011b). This matrix indicates the regional difference in surface area in the individual subject with respect to the common template where the two groups of subjects are registered. R^k values smaller than 1 indicate atrophic changes at a given vertex in preterm group, while values greater than 1 indicates enlargement at a particular vertex.

2.6. Relative pose analysis

To compute the relative position of each individual's lateral ventricles, we used a Procrustes alignment of each subject's structure in relation with a population-based template (Bossa and Olmos, 2006; Bossa et al., 2011a; Dryden and Mardia, 1998). The population-based template was calculated iteratively and then align to the subject's shape (Bossa et al., 2011a; Lao et al., 2014a, 2014b). For each structure, we computed a transformation matrix corresponding to the rotation, translation and scaling. The transformation matrix can be written as:

$$T = \begin{bmatrix} SRX & d \\ T & 1 \end{bmatrix} \quad (2)$$

where S is the scalar scaling factor, R is a 3 × 3 rotation matrix, and d is the translation vector $(x, y, z)^T$ (Bossa et al., 2011a). A schematic representation of the Procrustes transform applied to the left and right lateral ventricles is shown in Fig. 2. 13 sets of parameters were computed for each structure. Univariate parameters (9) comprised: logS, ||logR||, ||logd||, respectively representing the total scale, total rotation and total translation of each structure; θx,θy,θz, representing the 3 rotation parameters; and x, y, and z, representing the 3 translation parameters. Multivariate parameters (4) included: (θx, θy, θz); (x, y, z); (logS, ||logR||, ||logd||); and a combination of 7 parameters (1 scale, 3 rotations, 3 translations). For statistical computation, all transformations were centered on the center mass of the template, and projected onto the tangent plane at the origin of the manifold of transformations (Arsigny et al., 2006; Bossa and Olmos, 2006). As with the mTBM analyses, group analyses on the relative pose parameters were performed on post-conception age-covaried data using linear regression.

Between-group statistical comparisons were performed structure-wise on all 9 sets of univariate parameters (logS, ||logR||, ||logd||, θx, θy, θz, x, y, z) using univariate t-test. For the multivariate parameters ((θx, θy, θz), (x, y, z), (logS, ||logR||, ||logd||), combination of 7 parameters), the multivariate Hotelling's T^2 test was used. For each test, 10,000 permutations were performed to avoid the normal distribution assumption (Nichols and Holmes, 2002).

2.7. Surface and pose correlations

The structural relationship between the bilateral ventricles, the putamen and the thalamus described and discussed in Lao et al. (2014a, 2014b) and Shi et al. (2013b) were further investigated using Pearson's correlation analysis for both surface morphometry deformation and relative pose measures. For the surface deformation parameters, Pearson's correlations were performed between the determinant (surface area) of each vertex of the ventricles (LVent, RVent) and the total volume of the putamen (LPut, RPut) and the thalamus (LThal, RThal). We also ran two permutation tests on the surface-based correlations: a vertex-based one that allowed us to avoid normal distribution assumptions, and one over the total segmented images to correct for multiple comparisons (Lepore et al., 2008; Nichols and Holmes, 2002; Wang et al., 2011c). Similarly, to test for the relationship in terms of relative position between the two ventricles, and the two putamen and thalami, we computed Pearson's correlations on the pose parameters logS, ||logR||, and ||logd|| for each pair (LVent vs. LThal; LVent vs. LPuta; RVent vs. RThal; RVent vs. RPuta). For each correlation set, 10,000 permutations were computed to avoid the normal distribution assumption.

3. Results

3.1. Sociodemographic characteristics

Groups differences on demographic and birth data are displayed in Table 1. A t-test calculated on the birth weight and nonparametric Mann-Whitney U tests calculated on the gestational age revealed significant differences between preterm and full-term neonates (GA and Birth weight: $p < 0.001$), as expected. However, Mann–Whitney U tests revealed that the two groups were equivalent in terms of gender ($p = 0.657$), Apgar scores at 1 min ($p = 0.447$) and at 5 min ($p = 0.604$), and postnatal age at scan time ($p = 0.975$).

3.2. Surface morphometry results

Fig. 3a shows the results of the mTBM analysis on the ventricular surface morphometry of premature and full-term neonates. The p-value map shows significant group differences in the shape of the lateral ventricles with $p = 0.0005$, corrected for multiple comparisons. Fig. 3b show the direction of changes with values smaller than 1 indicating atrophic changes and values greater than 1 indicating enlargement in the preterm group. Local comparison analysis revealed broad areas of difference (at $p_t = 0.05$ level) where preterm neonates show significant ventricular enlargement. These regions are located primarily within the frontal horn and the body of the left ventricle, and more restricted, but significant, areas of differences on the temporal horn and body of the right ventricle.

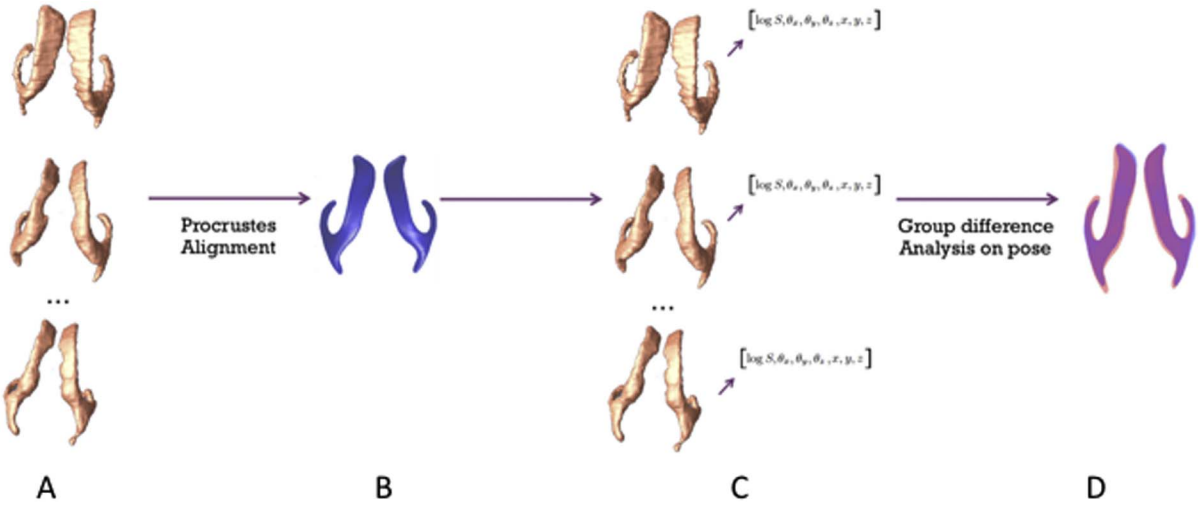

Fig. 2. Relative pose analysis pipeline. Individual shapes (A) are first Procrustes aligned to an average template shape (B), which results in a set of 7 parameters for each of subjects (C). Group analysis results (D) are then obtained through univariate and multivariate tests.

3.3. Relative position results

Results from the relative pose analysis (rotation, translation and scale) for all parameters are displayed in Table 2, and illustrated in Fig. 4. Significant differences between preterm and full-term neonates were found on the rotation parameter of the left ventricle, for both univariate (p = 0. 0165) and multivariate measures (p = 0.0499). For the right ventricle, only marginal differences were found on both the rotation (p = 0.0542) and translation (p = 0.0634) measures.

3.4. Correlations results

To further investigate the relationship between ventricular shape and pose, and the surrounding structures, we tested the surface morphometry and relative pose correlations between the ventricle and results previously found on the thalamus (Lao et al., 2014b) and putamen (Shi et al., 2013b). All p-values are computed using 10,000 permutations to correct for multiple comparisons, at 0.05 alpha level of significance.

3.4.1. Surface morphometry correlations

Fig. 5 shows the p-map of the correlational analysis on the surface morphometry of the ventricles and the surface of the putamen and thalamus (see Lao et al., 2014b and Shi et al., 2013b respectively, for additional details on the putamen and thalamus between-group analysis). The correlations on the shape of the bilateral ventricles and that of the bilateral thalamus and putamen were all nonsignificant (ventricle vs thalamus: p = 0.3320; ventricle vs putamen: p = 0.3866). Likewise, correlation analysis between these structures when tested within the left or the right hemispheres failed to reach significance. Corrected p-value after permutation tests were: (a) LVent vs. LThal: p = 0.8043; (b) LVent vs. LPuta: p = 0.3866: (c) RVent vs. RThal: p = 0.1357: (d)

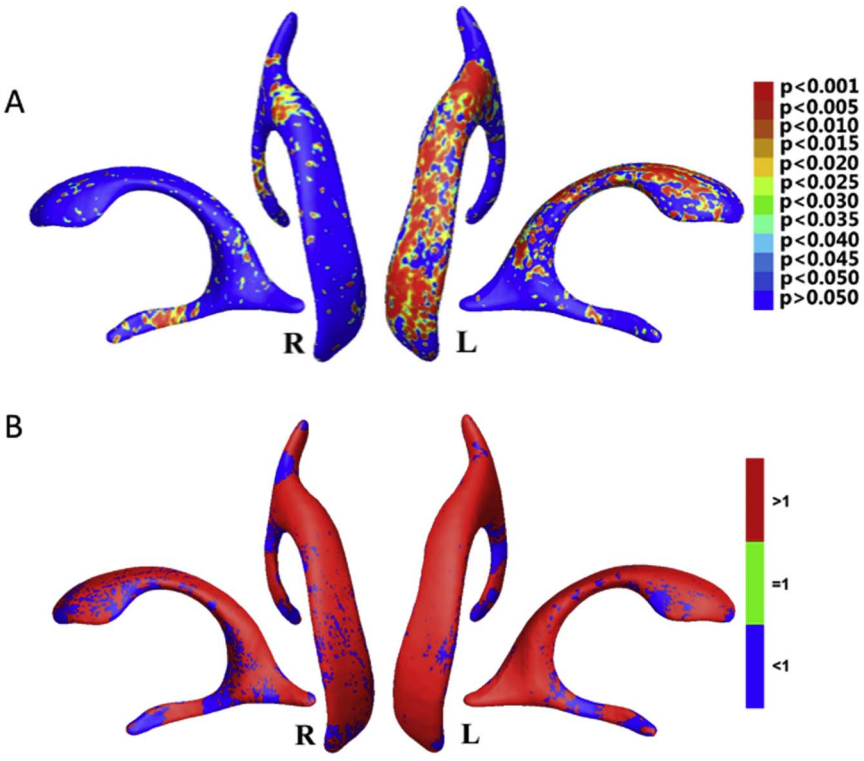

Fig. 3. The top row (A) show Statistical p-map representation of group differences detected between the preterm and term-born groups, using the smoothed and covaried mTBM (0.05 significance level for each surface vertex). The non-blue colors illustrate areas with statistically significant differences between the two groups. The bottom row (B) shows the direction of changes between groups. Values smaller than 1 (in blue) indicates atrophic changes at a given vertex in preterm group, while values greater than 1 (in red) indicate enlargement in the preterm group at the given vertex. (For interpretation of the references to color in this figure legend, the reader is referred to the web version of this article.)

Table 2
Results of the relative pose analysis.

Pose Parameters	LVent	RVent	Pose parameters (Cont)	LVent	RVent
logS	0.3979	0.8591	**||logR||**	0.5312	0.1421
θx	0.0606	0.0542	**||logd||**	0.5073	0.4515
θy	0.1395	0.5210	**(θx,θy,θz)**	0.0499	0.2123
θz	0.0165	0.4299	**(x, y, z)**	0.7387	0.1650
x	0.4644	0.0634	**(logS, ||logR||, ||logd||)**	0.784	0.5260
y	0.9694	0.3414	**All7parameters**	0.2405	0.1389
z	0.5519	0.9378			

p-valuecorrected formultiple comparisons using permutation tests.
Significant results (at 0.05 alpha level) are highlighted in blue; marginal differences arehighlighted in light grey.

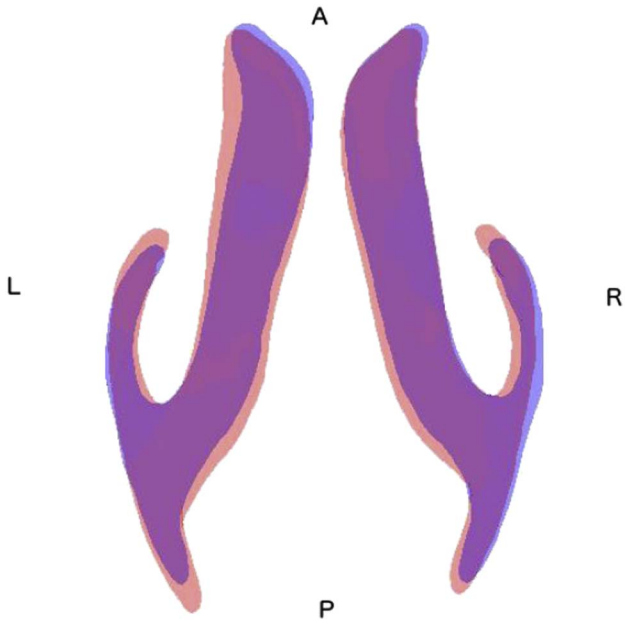

Fig. 4. 2D visualization of mean shapes averaged from preterm group (Red) and term group (Blue) for the left (LVent) and right (RVent) ventricle. Areas where the mean shapes of two groups overlaid appear in purple. (For interpretation of the references to color in this figure legend, the reader is referred to the web version of this article.)

RVent vs. RPuta: $p = 0.7296$.

3.4.2. Pose correlations

Fig. 6 shows the 3D representation of the relative position for the lateral ventricles, putamen and thalamus for the preterm (in red) and full-term (in blue) neonates, along with areas of shape overlapping between the two groups (in purple). Fig. 7 shows the correlation plots for the logS, ||logR||, and ||logd|| pose parameters between each structure (LVent vs. LTha, LVent vs. LPuta, RVent vs. RTha, and RVent vs. RPuta). The correlation coefficient and corrected *p*-values are displayed in Table 3 for each of the pose parameter tested (total scale, total rotation, total translation). Overall, significant correlations were found between each structure in terms of rotation (||logR||). Significant correlations were also found on the translation parameter (||log*d*||) between the left ventricle, and the left putamen and left thalamus, along with a significant correlation between the right ventricle and right putamen. Significant correlations on the scale parameter (logS) were found only between the left ventricle and left putamen.

4. Discussion

Here, we examined the morphological features of the lateral ventricles in a population of preterm and full-term born neonates. We applied a novel pipeline combining surface deformation and pose analysis to precisely characterize and localize ventricular abnormalities in these infants. Significant areas of differences were detected on the frontal horn and the body of the left ventricle, along with narrower differences on the temporal horn of the right ventricle. These results are consistent with prior works on the thalamus and putamen, showing changes in shape and pose located primarily within the left hemisphere (Lao et al., 2014b; Shi et al., 2013b). In addition, we found a significant shift in terms of rotation of the left ventricle in preterm neonates, with a trend for the right ventricle. This is also in line with previous findings showing significant pose alterations in the left thalamus and the right putamen, and trends in the left putamen (Lao et al., 2014b). Complementary to these results, we examined the relationship between changes in surface morphometry and pose parameters of the lateral ventricles, and those of the putamen and thalamus described previously. We found significant correlations between each of these structures in terms of rotation. We also measured significant correlations on the translation parameter between the left ventricle, and the left putamen and left thalamus, as well as between the right ventricle and right putamen. Significant correlation on the scale parameter was also found between the left ventricle and left putamen. Overall, these results further corroborate our previous works suggesting a left subcortical vulnerability to preterm birth. These results also show the interdependence between the ventricles and its surrounding structures as well as an atypical organization of the subcortical network in our sample of relatively healthy preterm neonates.

4.1. Impact of prematurity on subcortical organization

Here, pose abnormalities found in the lateral ventricles correlated significantly with those found in thalamus (Shi et al., 2013b) and putamen (Lao et al., 2014b). The ventricular pose differences in the present study and its relation to the pose differences in the thalamus and putamen, especially in terms of rotation and translation of the structures, suggest altered growth of the white matter tracts surrounding these structures. It is possible that altered growth, or dysmaturation, of the white matter is also found in synergy to impaired growth of the grey matter (Back, 2015; Back and Miller, 2014). The cerebral white and grey matter dysmaturation in preterm infants has been proposed to account for myelination and neural disturbance related to preterm birth, impacting the pre-oligodendrocytes (myelin promoting cells) and immature neurons development (Back, 2015; Back and Miller, 2014). This is further supported by our results showing group differences and structure inter-correlation in scale, or general volume, and shape surface, suggesting impaired neural development of the deep grey matter structures. These results need to be further validated in future work using diffusion based tractography analyses.

The effect of pose and surface changes of subcortical structures within the thalamo-cortical network in preterm infants have been previously proposed and discussed (Lao et al., 2014b; Shi et al., 2013b). The cortico-basal-thalamo-cortical networks is involved in a number of

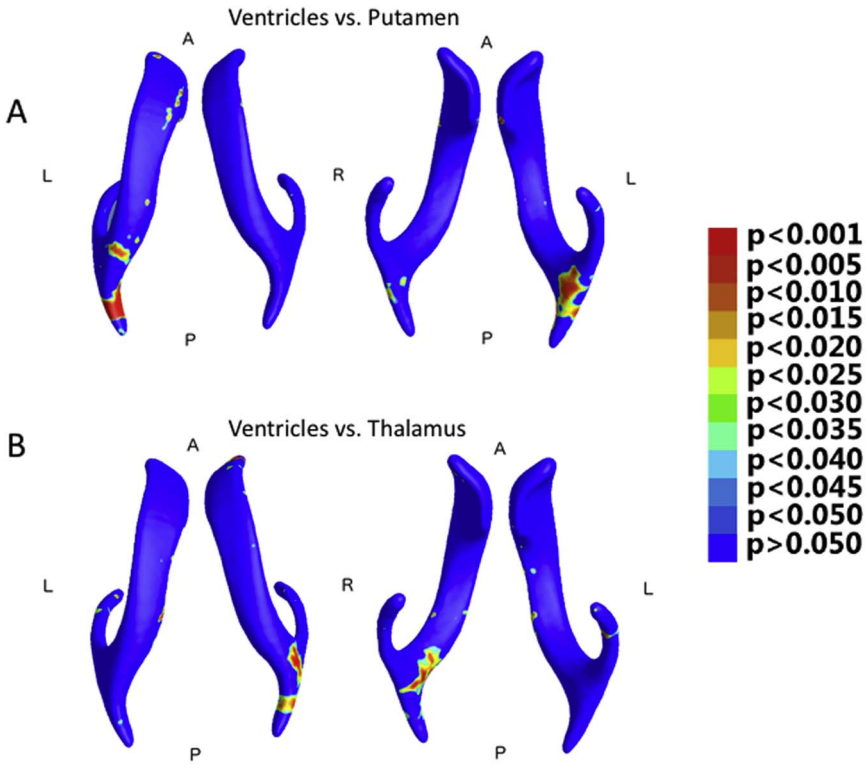

Fig. 5. 2D visualization of correlational analysis on vertex-wise surface morphometry between the ventricles and putamen (top row), and ventricles and thalami (bottom row) *p*-map at 0.05 significance level for each surface vertex.

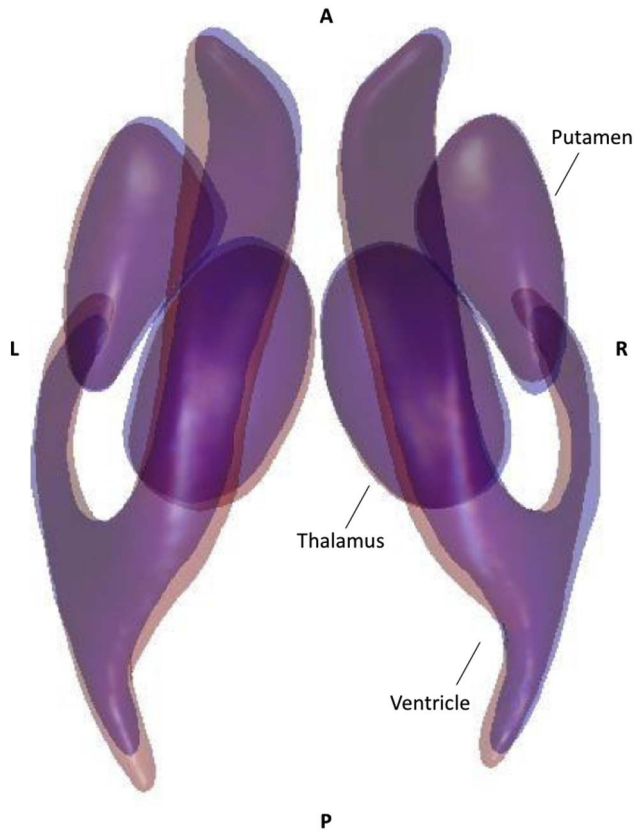

Fig. 6. 3D visualization of the pose of mean shapes averaged from preterm group (Red) and term group (Blue) for the lateral ventricles, thalamus and putamen. (For interpretation of the references to color in this figure, the reader is referred to the web version of this article.)

executives and goal-directed behaviors, such as executive, attention, and motor functioning (Ball et al., 2012; Draganski et al., 2008; Meng et al., 2016; Metzger et al., 2013). Compromised integrity in these systems have been described in adults and children born prematurely (Ball et al., 2012; Meng et al., 2016). As shown in the present study, the ventricular system may be involved in this network by its connections to the thalamus and putamen. However, to our knowledge, very few studies have investigated the relationships of the subcortical networks in the preterm neonates in relation to atypical development of the lateral ventricles. Boardman et al. (2006) found that preterm infants with diffuse white matter damage on diffusion weighted imaging also showed volumetric diminution within deep grey matter structures, along with a volumetric increase of the posterior horn of the lateral ventricle. These results also hint to an association between enlarged lateral ventricles, diffuse white matter injury, and structural abnormalities in deep grey matter structures in the preterm infant without visual evidence of acute brain injury. Nevertheless, additional work investigating the direct participation of the lateral ventricles to be cortico-basal-thalamo-cortical networks in the developing infant is needed, for instance combining mTBM, relative pose, and direct white matter tracking.

4.2. Asymmetric vulnerability of subcortical development

Although some of the significant differences and correlations found were located within the right hemisphere, it is interesting to note that we found greater patterns of ventricular alterations and correlations with the surrounding structures within the left hemisphere. Left hemispheric vulnerability has previously been reported in preterm born children affecting auditory information processing and language development (Gomot et al., 2007; Rushe et al., 2004). Likewise, atypical connectivity patterns were observed in preterm infants involving the left frontal and temporal cortical networks (Pannek et al., 2013). These regions are associated with working memory, verbal comprehension and higher cognitive functions, in which impairments are often detected at pre-school or school age in prematurely born children

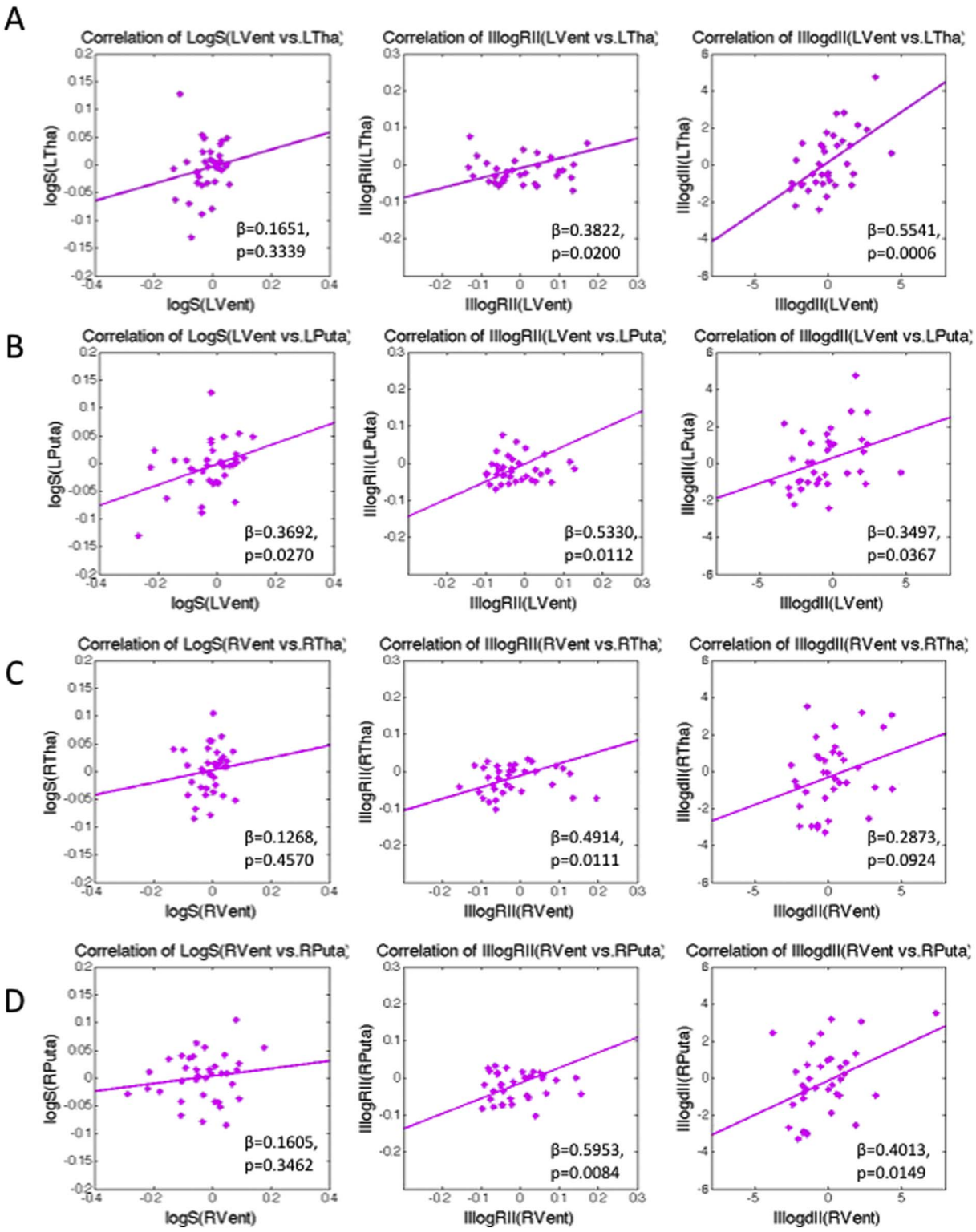

Fig. 7. Correlation plots between the ventricles and thalamus (A and C), and the ventricles and putamen (B and D) in the left (A and B) and right (C and D) hemispheres, tested using pose parameters: logS (left), ||logR|| (middle), ||logd|| (right).

(Anderson et al., 2011; Arpino et al., 2010; Sansavini et al., 2010). Recent evidences also suggest that left hemisphere myelination is more rapid than the right in many brain regions during early the perinatal period (Deoni et al., 2011). Region within the left hemisphere showing earlier onset of myelin development also appears to have slower subsequent myelination process than regions showing later myelination onset in the right hemisphere (Deoni et al., 2011). It is possible that preterm infants are more at risk of oligodendrocyte and myelination disturbances within the left hemisphere following perinatal injuries. Yet, the hemispheric vulnerability of subcortical network remains poorly investigated. Longitudinal and birth cohort studies that includes comprehensive neuroimaging, white matter tracking, neuropsychological, and behavioral assessments are needed to better understand and document the etiology and outcomes of this vulnerability.

Table 3
Correlation results based on pose parameters.

	logS	||logR||	||logd||
LVent vs. LTha	β=0.1651, p=0.3339	β=0.3822, p=0.0200	β=0.5541, p=0.0006
LVent vs. LPuta	β=0.3692, p=0.0270	β=0.5330, p=0.0112	β=0.3497, p=0.0367
RVent vs. RTha	β=0.1268, p=0.4570	β=0.4914, p=0.0111	β=0.2873, p=0.0924
RVent vs. RPuta	β=0.1605, p=0.3462	β=0.5953, p=0.0084	β=0.4013, p=0.0149

p-valuecorrected for multiple comparisons using permutation tests.
Significant results (at 0.05 alpha level) are highlighted in blue.

4.3. Ventricular abnormalities and neurodevelopment

Even in the absence visible brain injuries on the infants' MRI, isolated ventricular abnormalities are likely to be associated with subtle white matter damages that could not be identified on conventional neonatal ultrasounds or MRI analysis (Vollmer et al., 2006). However, the long-term impact of isolated ventricular abnormalities on neurodevelopment and cognitive functioning of preterm infants remains controversial. In infants with comorbidities such as cerebral palsy, bronchopulmonary dysplasia, intraventricular or cerebellar hemorrhage, significantly enlarged lateral ventricles, or ventriculomegaly, has been shown to increase the risk for moderate to severe neurodevelopmental sequelae (Bromley et al., 1991; Dyet et al., 2006; Maunu et al., 2010; Ment et al., 1999). Other studies have found little evidences of neurodevelopmental impairments on the longitudinal follow-up of neonates with isolated ventriculomegaly (Beeghly et al., 2010; Leitner et al., 2009; Ouahba et al., 2006). Yet, subtle white matter abnormalities were observed on the postnatal MRI of 18% of neonates with mild to moderate ventriculomegaly (Falip et al., 2007). Similarly, altered grey and white matter development was found in infants with isolated ventricular dilatation, along with reduced diffusion values in the thalamic radiation, sagittal stratum and corpus callosum, suggesting disrupted myelination process accompanying ventricular dilatation (Lockwood Estrin et al., 2016). Furthermore, about half of the infants with isolated ventriculomegaly also showed delay in language acquisition at 2 years of age. This is in line with a previous study showing significant impairments on the mental developmental index (MDI) of the Bayley scale of infant development (BSID-III) in children with isolated ventriculomegaly and poorer behavioral functioning in children with asymmetric ventricles (Sadan et al., 2007). In a follow-up assessment, lower performance was observed on attentional measure for the unilateral ventriculomegaly group, and slower writing speed was observed for the asymmetric ventricle group, although both groups performed within the norm on the global index of the Weschler (full-scale IQ) (Atad-Rapoport et al., 2015). It is possible that children with isolated unilateral ventriculomegaly or asymmetrical ventricles at birth may overcome most of their developmental or behavioral vulnerability in infancy. Nevertheless, the literature points to diverse and diffuse impairments in children with ventriculomegaly or atypical ventricular enlargement, and these children seems to remain at risk for cognitive limitations. Overall, these results highlight the need for more refined brain imaging technology capable to precisely characterize ventricular and subcortical abnormalities in term and preterm born infants.

4.4. Conclusion

To help characterize the effect of prematurity itself on anatomical subcortical brain development, we used advanced algorithms capable to precisely quantify and localize structural surface deformation in otherwise “healthy” preterm infants. Our multivariate analysis (mTBM) has been tested and validated in both children and adults (Lao et al., 2017a, 2017b; Lao et al., 2014b; Shi et al., 2013b; Wang et al., 2011a, 2011b). Previous findings comparing mTBM with more common univariate versions of TBM revealed consistent areas of group differences between these techniques, although the former provided higher effect sizes even with relatively small sample size, thus increased statistical power (Lao et al., 2017a, 2017b; Lao et al., 2014b; Shi et al., 2013b; Wang et al., 2010). In addition, our method combine multivariate surface based morphometry and complementary relative pose analysis to precisely locate and quantify abnormalities on specific subcortical structures (Bossa and Olmos, 2006; Bossa et al., 2011a, 2011b; Lao et al., 2014a; Lao et al., 2014b). In our study, group-analysis on the rotation, translation and scale parameters confirmed the association of prematurity on the ventricular abnormalities in our sample and provided comprehensive information of the ventricular system morphometry in preterm and full-term neonates. Overall, the complementarity of the information provided by the surface and pose analysis may help to indicate abnormal brain growth, particularly in populations were shifts in pose of a given structure is likely to happen (for instance, in case of abnormal development or degenerative patterns).

4.5. Methodological limitations and future directions

There are several limitations to our study. First, childhood is often characterized by high inter-individual variability, especially regarding functional and structural brain maturation. Because of the small sample size of this study, inference about children neurodevelopment is limited. Secondly, longitudinal information about this cohort of neonates is not currently available and factors such as treatment and medical or psychopharmacologic intervention were not investigated in this study. Larger sample size and longitudinal follow-up could provide more information on the atypical development subcortical structures, both in terms of pose and surface measurement, in preterm and full-term born children. Furthermore, a longitudinal follow-up could allow us to correlate the above results with long-term clinical outcomes and to further investigate other possible risk factors, such as the impact of associated early brain injuries, degrees of prematurity, or other medical conditions. The methods described above may be applied to study group differences in cortical and subcortical structure in various clinical population and in subjects of different ages. It would also be of particular interest to further investigate the effectiveness of various treatments and interventions on the long-term cerebral development of the preterm infant.

Acknowledgment

We thank for the participation of families from Children's Hospital Los Angeles and Children's Hospital of Pittsburgh UPMC. This work was supported by NIH grant K23NS063371 and NIH/NCRR/NCATS SC CTSI grant UL1 RR031986 (AP), NIH grants R21AG049216 and RF1AG051710 (YW and JS), as well a CHIR research fellowship (NP).

References

Allin, M., Henderson, M., Suckling, J., Nosarti, C., Rushe, T., Fearon, P., ... Murray, R., 2004. Effects of very low birthweight on brain structure in adulthood. Dev. Med. Child Neurol. 46 (1), 46–53. http://dx.doi.org/10.1017/S0012162204000088.
Allin, M.P.G., Kontis, D., Walshe, M., Wyatt, J., Barker, G.J., Kanaan, R., ... Nosarti, C., 2011. White matter and cognition in adults who were born preterm. PLoS One 6 (10),

e24525. http://dx.doi.org/10.1371/journal.pone.0024525.
Anderson, P.J., De Luca, C.R., Hutchinson, E., Spencer-Smith, M.M., Roberts, G., Doyle, L.W., 2011. Attention problems in a representative sample of extremely preterm/extremely low birth weight children. Dev. Neuropsychol. 36 (1), 57–73. http://dx.doi.org/10.1080/87565641.2011.540538.
Arpino, C., Compagnone, E., Montanaro, M.L., Cacciatore, D., Luca, A. De, Cerulli, A., ... Curatolo, P., 2010. Preterm birth and neurodevelopmental outcome: a review. Childs Nerv. Syst. http://dx.doi.org/10.1007/s00381-010-1125-y.
Arsigny, V., Fillard, P., Pennec, X., Ayache, N., 2006. Log-Euclidean metrics for fast and simple calculus on diffusion tensors. Magn. Reson. Med. 56 (2), 411–421. http://dx.doi.org/10.1002/mrm.20965.
Atad-Rapoport, M., Schweiger, A., Lev, D., Sadan-Strul, S., Malinger, G., Lerman-Sagie, T., 2015. Neuropsychological follow-up at school age of children with asymmetric ventricles or unilateral ventriculomegaly identified in utero. BJOG 122, 932–938. An International Journal of Obstetrics and Gynaecology. http://dx.doi.org/10.1111/1471-0528.13312.
Back, S.A., 2015. Brain injury in the preterm infant: new horizons for pathogenesis and prevention. Pediatr. Neurol. 53 (3), 185–192. http://dx.doi.org/10.1016/j.pediatrneurol.2015.04.006. (Brain).
Back, S.A., Miller, S.P., 2014. Brain injury in premature neonates: A primary cerebral dysmaturation disorder? Ann. Neurol. http://dx.doi.org/10.1002/ana.24132.
Ball, G., Boardman, J.P., Rueckert, D., Aljabar, P., Arichi, T., Merchant, N., ... Counsell, S.J., 2012. The effect of preterm birth on thalamic and cortical development. Cereb. Cortex 22 (5), 1016–1024. http://dx.doi.org/10.1093/cercor/bhr176.
Beeghly, M., Ware, J., Soul, J., Du Plessis, A., Khwaja, O., Senapati, G.M., ... Levine, D., 2010. Neurodevelopmental outcome of fetuses referred for ventriculomegaly. Ultrasound Obstet. Gynecol. 35 (4), 405–416. http://dx.doi.org/10.1002/uog.7554.
Boardman, J.P., Counsell, S.J., Rueckert, D., Kapellou, O., Bhatia, K.K., Aljabar, P., ... Edwardsa, A.D., 2006. Abnormal deep grey matter development following preterm birth detected using deformation-based morphometry. NeuroImage 32 (1), 70–78. http://dx.doi.org/10.1016/j.neuroimage.2006.03.029.
Boardman, J.P., Craven, C., Valappil, S., Counsell, S.J., Dyet, L.E., Rueckert, D., ... Edwards, a D., 2010. A common neonatal image phenotype predicts adverse neurodevelopmental outcome in children born preterm. NeuroImage 52 (2), 409–414. http://dx.doi.org/10.1016/j.neuroimage.2010.04.261.
Bossa, M.N., Olmos, S., 2006. Statistical model of similarity transformations: building a multi-object pose model of brain structures. In: Proceedings of the IEEE Computer Society Conference on Computer Vision and Pattern Recognition. Vol. 2006http://dx.doi.org/10.1109/CVPRW.2006.198.
Bossa, M., Zacur, E., Olmos, S., 2011a. Statistical analysis of relative pose information of subcortical nuclei: Application on ADNI data. NeuroImage 55 (3), 999–1008. http://dx.doi.org/10.1016/j.neuroimage.2010.12.078.
Bossa, M., Zacur, E., Olmos, S., The Alzheimer's Disease Neuroimaging Initiative, 2011b. Statistical analysis of relative pose information of subcortical nuclei: Application on ADNI data. NeuroImage 55 (3), 999–1008. http://dx.doi.org/10.1016/j.neuroimage.2010.12.078.Statistical.
Bromley, B., Frigoletto, F.D., Benacerraf, B.R., 1991. Mild fetal lateral cerebral ventriculomegaly: clinical course and outcome. Am. J. Obstet. Gynecol. 164 (3), 863–867. http://dx.doi.org/10.1016/0002-9378(91)90530-5.
Chollet, M.B., Aldridge, K., Pangborn, N., Weinberg, S.M., DeLeon, V.B., 2014. Landmarking the brain for geometric morphometric analysis: an error study. PLoS One 9 (1). http://dx.doi.org/10.1371/journal.pone.0086005.
Chung, M.K., Robbins, S.M., Dalton, K.M., Davidson, R.J., Alexander, A.L., Evans, A.C., 2005. Cortical thickness analysis in autism with heat kernel smoothing. NeuroImage 25 (4), 1256–1265. http://dx.doi.org/10.1016/j.neuroimage.2004.12.052.
Counsell, S.J., Edwards, A.D., Chew, A.T.M., Anjari, M., Dyet, L.E., Srinivasan, L., ... Cowan, F.M., 2008. Specific relations between neurodevelopmental abilities and white matter microstructure in children born preterm. Brain 131, 3201–3208. A Journal of Neurology. http://dx.doi.org/10.1093/brain/awn268.
Deoni, S.C.L., Mercure, E., Blasi, A., Gasston, D., Thomson, A., Johnson, M., ... Murphy, D.G.M., 2011. Mapping infant brain myelination with magnetic resonance imaging. J. Neurosci. 31 (2), 784–791. http://dx.doi.org/10.1523/JNEUROSCI.2106-10.2011.
Draganski, B., Kherif, F., Kloppel, S., Cook, P.A., Alexander, D.C., Parker, G.J., ... Frackowiak, R.S., 2008. Evidence for segregated and integrative connectivity patterns in the human *Basal Ganglia*. J. Neurosci. 28 (28), 7143–7152. http://dx.doi.org/10.1523/JNEUROSCI.1486-08.2008.
Dryden, I.L., Mardia, K.V., 1998. Statistical shape analysis. J. Hum. Evol. 4 (3), 376. http://dx.doi.org/10.1006/jhev.1999.0391.
Dyet, L.E., Kennea, N., Counsell, S.J., Maalouf, E.F., Ajayi-Obe, M., Duggan, P.J., ... Edwards, A.D., 2006. Natural history of brain lesions in extremely preterm infants studied with serial magnetic resonance imaging from birth and neurodevelopmental assessment. Pediatrics 118 (2), 536–548. http://dx.doi.org/10.1542/peds.2005-1866.
Falip, C., Blanc, N., Maes, E., Zaccaria, I., Oury, J.F., Sebag, G., Garel, C., 2007. Postnatal clinical and imaging follow-up of infants with prenatal isolated mild ventriculomegaly: a series of 101 cases. Pediatr. Radiol. 37 (10), 981–989. http://dx.doi.org/10.1007/s00247-007-0582-2.
Gomot, M., Bruneau, N., Laurent, J., Barthélémy, C., Saliba, E., 2007. Left temporal impairment of auditory information processing in prematurely born 9-year-old children: an electrophysiological study. Int. J. Psychophysiol. 64, 123–129. http://dx.doi.org/10.1016/j.ijpsycho.2007.01.003.
Hamilton, R.S., 1988. The Ricci flow on surfaces. Contemp. Math. 71, 237–262.
Han, X., Xu, C., Prince, J.L., 2003. A topology preserving level set method for geometric deformable models. IEEE Trans. Pattern Anal. Mach. Intell. 25 (6), 755–768. http://dx.doi.org/10.1109/TPAMI.2003.1201824.
Hoppe, H., 1996. Progressive meshes. In: Proceedings of the 23rd Annual Conference on Computer Graphics and Interactive Techniques - SIGGRAPH '96, pp. 99–108. http://dx.doi.org/10.1145/237170.237216.
Hotelling, H., 1931. The generalization of Student's ratio. Ann. Math. Stat. 2, 360–378.
Isaacs, E.B., Lucas, A., Chong, W.K., Wood, S.J., Johnson, C.L., Marshall, C., ... Gadian, D.G., 2000. Hippocampal volume and everyday memory in children of very low birth weight. Pediatr. Res. 47, 713–720.
Kesler, S.R., Ment, L.R., Vohr, B., Pajot, S.K., Schneider, K.C., Katz, K.H., ... Reiss, A.L., 2004. Volumetric analysis of regional cerebral development in preterm children. Pediatr. Neurol. 31 (5), 318–325. http://dx.doi.org/10.1016/j.pediatrneurol.2004.06.008.
Lao, Y., Dion, L.-A., Gilbert, G., Bouchard, M.F., Rocha, G., Wang, Y., ... Saint-Amour, D., 2017a. Mapping the basal ganglia alterations in children chronically exposed to manganese. Sci. Rep. 7 (February), 41,804. http://dx.doi.org/10.1038/srep41804.
Lao, Y., Nguyen, B., Tsao, S., Gajawelli, N., Law, M., Chui, H., ... Leporé, N., 2017b. A T1 and DTI fused 3D corpus callosum analysis in MCI subjects with high and low cardiovascular risk profile. NeuroImage 14, 298–307 Clinical.
Lao, Y., Shi, J., Wang, Y., Ceschin, R., Hwang, D., Nelson, M.D., ... Leporé, N., 2014a. Statistical analysis of relative pose of the thalamus in preterm neonates. In: 2nd International Workshop on Clinical Image-Based Procedures: Translational Research in Medical Imaging, CLIP 2013 - Held in Conjunction with MICCAI 2013, pp. 1–9. http://dx.doi.org/10.1007/978-3-319-05666-1_1.
Lao, Y., Wang, Y., Shi, J., Ceschin, R., Nelson, M.D., Panigrahy, A., Leporé, N., 2014b. Thalamic alterations in preterm neonates and their relation to ventral striatum disturbances revealed by a combined shape and pose analysis. Brain Struct. Funct. http://dx.doi.org/10.1007/s00429-014-0921-7.
Leitner, Y., Stolar, O., Rotstein, M., Toledano, H., Harel, S., Bitchonsky, O., ... Ben-Sira, L., 2009. The neurocognitive outcome of mild isolated fetal ventriculomegaly verified by prenatal magnetic resonance imaging. Am. J. Obstet. Gynecol. 201 (2). http://dx.doi.org/10.1016/j.ajog.2009.04.031.
Lepore, N., Brun, C., Chou, Y.-Y., Chiang, M.-C., Dutton, R.A., Hayashi, K.M., ... Thompson, P.M., 2008. Multivariate statistics on deformation tensors. IEEE Trans. Med. Imaging 27 (1), 129–141. http://dx.doi.org/10.1109/TMI.2007.906091.Generalized.
Lockwood Estrin, G., Kyriakopoulou, V., Makropoulos, A., Ball, G., Kuhendran, L., Chew, A., ... Rutherford, M.A., 2016. Altered white matter and cortical structure in neonates with antenatally diagnosed isolated ventriculomegaly. NeuroImage 11, 139–148. Clinical. http://dx.doi.org/10.1016/j.nicl.2016.01.012.
Loop, C., 1987. Smooth subdivision surfaces based on triangles. ACM Siggraph Retrieved from. http://www.citeulike.org/group/5490/article/2864922.
Lorensen, W.E., Cline, H.E., 1987. Marching cubes: a high resolution 3D surface construction algorithm. Proceedings of the 14th Annual Conference on Computer Graphics and Interactive Techniques - SIGGRAPH '87 21 (4), 163–169. http://dx.doi.org/10.1145/37402.37422.
Maalouf, E.F., Duggan, P.J., Rutherford, M.A., Counsell, S.J., Fletcher, A.M., Battin, M., ... Edwards, A.D., 1999. Magnetic resonance imaging of the brain in a cohort of extremely preterm infants. J. Pediatr. 135, 351–357. http://dx.doi.org/10.1016/S0022-3476(99)70133-2.
Maunu, J., Lehtonen, L., Lapinleimu, H., Matomäki, J., Munck, P., Rikalainen, H., ... Haataja, L., 2010. Ventricular dilatation in relation to outcome at 2 years of age in very preterm infants: a prospective Finnish cohort study. Dev. Med. Child Neurol. 53 (1), 48–54. http://dx.doi.org/10.1111/j.1469-8749.2010.03785.x.
Maunu, J., Parkkola, R., Rikalainen, H., Lehtonen, L., Haataja, L., Lapinleimu, H., PIPARI Group, 2009. Brain and ventricles in very low birth weight infants at term: a comparison among head circumference, ultrasound, and magnetic resonance imaging. Pediatrics 123 (2), 617–623. http://dx.doi.org/10.1542/peds.2007-3264.
Meng, C., Bauml, J.G., Daamen, M., Jaekel, J., Neitzel, J., Scheef, L., ... Sorg, C., 2016. Extensive and interrelated subcortical white and gray matter alterations in preterm-born adults. Brain Struct. Funct. 221 (4), 2109–2121. http://dx.doi.org/10.1007/s00429-015-1032-9.
Ment, L.R., Vohr, B., Allan, W., Westerveld, M., Katz, K.H., Schneider, K.C., Makuch, R.W., 1999. The etiology and outcome of cerebral ventriculomegaly at term in very low birth weight preterm infants. Pediatrics 104 (2), 243–248. http://dx.doi.org/10.1542/peds.104.2.243.
Metzger, C.D., Van der Werf, Y.D., Walter, M., 2013. Functional mapping of thalamic nuclei and their integration into cortico-striatal-thalamo-cortical loops via ultra-high resolution imaging-from animal anatomy to in vivo imaging in humans. Front. Neurosci. http://dx.doi.org/10.3389/fnins.2013.00024.
Nichols, T.E., Holmes, A.P., 2002. Nonparametric permutation tests for functional neuroimaging: a primer with examples. Hum. Brain Mapp. 15 (1), 1–25. http://dx.doi.org/10.1002/hbm.1058.
Nosarti, C., Al-Asady, M.H.S., Frangou, S., Stewart, A.L., Rifkin, L., Murray, R.M., 2002. Adolescents who were born very preterm have decreased brain volumes. Brain 125, 1616–1623. A Journal of Neurology. http://dx.doi.org/10.1093/brain/awf157.
Nosarti, C., Giouroukou, E., Healy, E., Rifkin, L., Walshe, M., Reichenberg, A., ... Murray, R.M., 2008. Grey and white matter distribution in very preterm adolescents mediates neurodevelopmental outcome. Brain 131, 205–217. http://dx.doi.org/10.1093/brain/awm282.
Nosarti, C., Nam, K.W., Walshe, M., Murray, R.M., Cuddy, M., Rifkin, L., Allin, M.P.G., 2014. Preterm birth and structural brain alterations in early adulthood. NeuroImage 6, 180–191. Clinical. http://dx.doi.org/10.1016/j.nicl.2014.08.005.
Ouahba, J., Luton, D., Vuillard, E., Garel, C., Gressens, P., Blanc, N., ... Oury, J.F., 2006. Prenatal isolated mild ventriculomegaly: outcome in 167 cases. BJOG 113 (9), 1072–1079. An International Journal of Obstetrics and Gynaecology. http://dx.doi.org/10.1111/j.1471-0528.2006.01050.x.
Pannek, K., Hatzigeorgiou, X., Colditz, P.B., Rose, S., 2013. Assessment of structural connectivity in the preterm brain at term equivalent age using diffusion MRI and T2

relaxometry: a network-based analysis. PLoS One 8 (8), e68593. http://dx.doi.org/10.1371/journal.pone.0068593.

Rushe, T.M., Temple, C.M., Rifkin, L., Woodruff, P.W.R., Bullmore, E.T., Stewart, A.L., ... Murray, R.M., 2004. Lateralisation of language function in young adults born very preterm. Arch. Dis. Child Fetal Neonatal Ed. 89 (2), 112F–1118. http://dx.doi.org/10.1136/adc.2001.005314.

Sadan, S., Malinger, G., Schweiger, A., Lev, D., Lerman-Sagie, T., 2007. Neuropsychological outcome of children with asymmetric ventricles or unilateral mild ventriculomegaly identified in utero. BJOG 114 (5), 596–602. An International Journal of Obstetrics and Gynaecology. http://dx.doi.org/10.1111/j.1471-0528.2007.01301.x.

Sansavini, A., Guarini, A., Justice, L.M., Savini, S., Broccoli, S., Alessandroni, R., Faldella, G., 2010. Does preterm birth increase a child's risk for language impairment? Early Hum. Dev. 86 (12), 765–772. http://dx.doi.org/10.1016/j.earlhumdev.2010.08.014.

Shi, J., Stonnington, C.M., Thompson, P.M., Chen, K., Gutman, B., Reschke, C., ... Wang, Y., 2015. Studying ventricular abnormalities in mild cognitive impairment with hyperbolic Ricci flow and tensor-based morphometry. NeuroImage 104, 1–20. http://dx.doi.org/10.1016/j.neuroimage.2014.09.062.

Shi, J., Thompson, P.M., Gutman, B., Wang, Y., 2013a. Surface fluid registration of conformal representation: Application to detect disease burden and genetic influence on hippocampus. NeuroImage 78, 111–134. http://dx.doi.org/10.1016/j.neuroimage.2013.04.018.

Shi, J., Wang, Y., Ceschin, R., An, X., 2012. Surface fluid registration and multivariate tensor-based morphometry in newborns-the effects of prematurity on the putamen. In: Signal & Information Processing Association Annual Summit and Conference (APSIPA ASC), Hollywood (CA). Retrieved from. http://gsl.lab.asu.edu/archive/apsipa_12.pdf.

Shi, J., Wang, Y., Ceschin, R., An, X., Lao, Y., Vanderbilt, D., ... Lepore, N., 2013b. A multivariate surface-based analysis of the putamen in premature newborns: regional differences within the ventral striatum. PLoS One 8 (7), e66736. http://dx.doi.org/10.1371/journal.pone.0066736.

Skranes, J., Vangberg, T.R., Kulseng, S., Indredavik, M.S., Evensen, K.A.I., Martinussen, M., ... Brubakk, A.-M., 2007. Clinical findings and white matter abnormalities seen on diffusion tensor imaging in adolescents with very low birth weight. Brain 130, 654–666. http://dx.doi.org/10.1093/brain/awm001.

Thompson, D.K., Adamson, C., Roberts, G., Faggian, N., Wood, S.J., Warfield, S.K., ... Inder, T.E., 2013. Hippocampal shape variations at term equivalent age in very preterm infants compared with term controls: perinatal predictors and functional significance at age 7. NeuroImage 70, 278–287. http://dx.doi.org/10.1016/j.neuroimage.2012.12.053.

Vollmer, B., Roth, S., Riley, K., Sellwood, M.W., Baudin, J., Neville, B.G., Wyatt, J.S., 2006. Neurodevelopmental outcome of preterm infants with ventricular dilatation with and without associated haemorrhage. Dev. Med. Child Neurol. 48 (5), 348–352. http://dx.doi.org/10.1017/s0012162206000764.

Wang, Y., Panigrahy, A., Ceschin, R., Liu, S., Thompson, P.M., Leporé, N., 2011a. Surface morphometry of subcortical structures in premature neonates. In: Annual Meeting of International Society for ISMRM, (Québec, Canada).

Wang, Y., Panigrahy, A., Shi, J., Ceschin, R., Marvin, D., Gutman, B., ... Lepor, N., 2011b. Surface Multivariate Tensor-based Morphometry on Premature Neonates: A Pilot Study. In: MICCAI Workshop on Image Analysis of Human Brain Development, (Toronto, Canada).

Wang, Y., Song, Y., Rajagopalan, P., An, T., Liu, K., Chou, Y.Y., ... The Alzheimer's Disease Neuroimaging Initiative, 2011c. Surface-based TBM boosts power to detect disease effects on the brain: an N = 804 ADNI study. NeuroImage 56 (4), 1993–2010. http://dx.doi.org/10.1016/j.neuroimage.2011.03.040.

Wang, Y., Yin, X., Zhang, J., Gu, X., Chan, T.F., Thompson, P.M., Yau, S.T., 2008. Brain mapping with the Ricci flow conformal parameterization and multivariate statistics on deformation tensors. In: 2nd MICCAI Workshop on Mathematical Foundations of Computational Anatomy, pp. 36–47. Retrieved from. http://citeseerx.ist.psu.edu/viewdoc/download?doi=10.1.1.142.207&rep=rep1&type=pdf.

Wang, Y., Zhang, J., Gutman, B., Chan, T.F., Becker, J.T., Aizenstein, H.J., ... Thompson, P.M., 2010. Multivariate tensor-based morphometry on surfaces: Application to mapping ventricular abnormalities in HIV/AIDS. NeuroImage 49 (1), 2141–2157. http://dx.doi.org/10.1016/j.neuroimage.2009.10.086.

Woo Nam, K., Castellanos, N., Simmons, A., Froudist-Walsh, S., Allin, M.P., Walshe, M., ... Nosarti, C., 2015. Alterations in cortical thickness development in preterm-born individuals: implications for high-order cognitive functions. NeuroImage 115, 64–75. http://dx.doi.org/10.1016/j.neuroimage.2015.04.015.

Yushkevich, P., Piven, J., Cody, H., Ho, S., 2006. User-guided level set segmentation of anatomical structures with ITK-SNAP. NeuroImage 31 (3), 1116–1128.

Zeng, W., Samaras, D., Gu, X.D., 2010. Ricci flow for 3D shape analysis. IEEE Trans. Pattern Anal. Mach. Intell. 32 (4), 662–677. http://dx.doi.org/10.1109/TPAMI.2009.201.